

Charge-memory polaron effect in molecular junctions

Dmitry A. Ryndyk¹, Pino D'Amico¹, Gianaurelio Cuniberti², and Klaus Richter¹

¹*Institute for Theoretical Physics, University of Regensburg, D-93040 Regensburg, Germany*

²*Institute for Material Science and Max Bergmann Center of Biomaterials, Dresden University of Technology, D-01062 Dresden, Germany*

(Dated: February 20, 2008)

The charge-memory effect, bistability and switching between charged and neutral states of a molecular junction, as observed in recent STM experiments, is considered within a minimal polaron model. We show that in the case of strong electron-vibron interaction the rate of spontaneous quantum switching between charged and neutral states is exponentially suppressed at zero bias voltage but can be tuned through a wide range of finite switching timescales upon changing the bias. We further find that, while junctions with symmetric voltage drop give rise to random switching at finite bias, asymmetric junctions exhibit hysteretic behavior enabling controlled switching. Lifetimes and charge-voltage curves are calculated by the master equation method for weak coupling to the leads and at stronger coupling by the equation-of-motion method for nonequilibrium Green functions.

Memory effects and switching at the molecular scale are in the focus of present experimental and theoretical studies within molecular electronics [1, 2, 3, 4, 5, 6, 7]. Beside stochastic switching in single-molecule junctions [4], recent STM experiments [2, 3] show multistability of neutral and charged states of single metallic atoms coupled to a metallic substrate through a thin insulating ionic film. The switching was performed by the application of a finite voltage to the STM tip and was explained by the large ionic polarizability of the film [2].

The coupling of a charge to the displacement of ions in the film can be treated as an electron-vibron interaction. If the energy of the *unoccupied* electron level *without electron-vibron interaction* is ϵ_0 , the *occupied* (charged) state of the *interacting system* will have the energy $\epsilon_1 = \epsilon_0 - \epsilon_p$, where ϵ_p is so-called polaron shift (or recombination energy). Neutral and charged (polaron) states correspond to local minimums of the potential energy surface and are metastable, if the electron-vibron interaction is strong enough. Applying an external voltage, one can change the state of this bistable system, an effect that is accompanied by hysteretic charge-voltage and current-voltage curves. In this approximation it is not necessary to include Coulomb interaction explicitly, though one can additionally incorporate charging effects.

It was suggested [8, 9] that bistability between charged and neutral states can be accounted for in a single-level model, when one electron level is coupled to one vibration (Fig. 1). The same problem was also considered in Refs. [10, 11], however with the conclusion that quantum switching between bistable states results in telegraph noise at finite voltage rather than in a memory effect. In this Letter we show that there is no contradiction among these two pictures, taking into account the time-scale of the switching process. Indeed, the switching time τ between the two states of interest should be compared with the characteristic time of the external voltage sweeping, $\tau_s \sim V(t)/(dV(t)/dt)$. For $\tau \gg \tau_s$, quantum switching can be neglected and hysteresis can be observed, while

in the opposite limit, $\tau \ll \tau_s$, the averaging removes the hysteresis. We calculate the charge-voltage curves and describe the full crossover between two regimes.

The Hamiltonian of the single-level polaron model is

$$\hat{H} = (\epsilon_0 + e\varphi_0)d^\dagger d + \omega_0 a^\dagger a + \lambda (a^\dagger + a) d^\dagger d + \sum_{ik} [(\epsilon_{ik} + e\varphi_i)c_{ik}^\dagger c_{ik} + (V_{ik}c_{ik}^\dagger d + h.c.)], \quad (1)$$

where the first three terms describe the free electron state, the free vibron of frequency ω_0 ($\hbar = 1$) and the electron-vibron interaction. The further terms are the Hamiltonian of the leads and the tunneling coupling ($i = L, R$ is the lead index, k labels electron states). The electrical potential φ_0 plays an important role in transport at finite bias voltages $V = \varphi_L - \varphi_R$ between

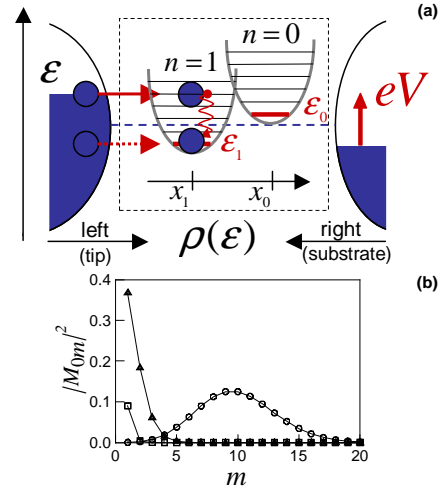


Figure 1: (Color online) (a) The energy diagram of the single-level electron-vibron model, coupled to left and right lead (or tip and substrate in the case of STM). (b) Franck-Condon matrix elements M_{0m} for weak ($g = 0.1$, squares), intermediate ($g = 1$, triangles), and strong ($g = 10$, circles) interaction.

the left and right electrical potentials. φ_0 describes the shift of the molecular level by the bias voltage and can be written as $\varphi_0 = \varphi_R + \eta(\varphi_L - \varphi_R)$, $\eta \in [0, 1]$ [12].

The coupling to the leads is characterized by the level-width function $\Gamma_i(\epsilon) = 2\pi \sum_k |V_{ik}|^2 \delta(\epsilon - \epsilon_{ik})$, where the coupling V_{ik} is assumed to be energy-independent (wide-band limit). The full level broadening is given by the sum $\Gamma = \Gamma_L + \Gamma_R$.

Consider first the case of very weak coupling to the leads, $\Gamma \ll \omega_0, \epsilon_p$. Using the polaron (Lang-Firsov) [13, 14, 15] canonical transformation, it is easy to show that the eigenstates of the *isolated system* ($\Gamma = 0$) are

$$|\psi_{nm}\rangle = e^{-\frac{\lambda}{\omega_0}(a^\dagger - a)d^\dagger d} (d^\dagger)^n \frac{(a^\dagger)^m}{\sqrt{m!}} |0\rangle \quad (2)$$

with the energies

$$E_{nm} = \epsilon_1 n + \omega_0 m, \quad \epsilon_1 = \epsilon_0 - \frac{\lambda^2}{\omega_0}, \quad \epsilon_p = \frac{\lambda^2}{\omega_0}. \quad (3)$$

When the system is weakly coupled to the leads, the polaron representation, Eqs. (2,3), is a convenient starting point. n denotes the number of electrons, while the quantum number m characterizes vibronic eigenstates, which are superpositions of states with different number of bare vibrons. The qualitative picture of the sequential tunneling through a polaronic state is given in Fig. 1(a). Here the potential energies of the neutral and charged states are sketched as a function of the vibronic coordinate x . When the external voltage is applied, the energy levels are shifted depending on the asymmetry parameter η . It should be noted that this type of the energy diagram is quite general for charge-controlled bistable systems.

In the sequential tunneling regime the master equation for the probability $p_{nm}(t)$ to find the system in one of the polaron eigenstates (2) can be written as [16, 17, 18]

$$\frac{dp_{nm}}{dt} = \sum_{n'm'} \Gamma_{mm'}^{nn'} p_{n'm'} - \sum_{n'm'} \Gamma_{m'm}^{n'n} p_{nm} + I^V[p]. \quad (4)$$

Here the first term describes the tunneling transition *into the state* $|n, m\rangle$ and the second term the transition *out of the state* $|n, m\rangle$. $I^V[p]$ is the vibron scattering integral describing the relaxation of vibrons to equilibrium. The transition rates $\Gamma_{mm'}^{nn'}$ are found from the tunneling Hamiltonian (the last term in Eq. (1)). Taking into account all possible single-electron tunneling processes, we obtain the incoming and outgoing tunneling rates at zero bias voltage as

$$\Gamma_{mm'}^{10} = \sum_{i=L,R} \Gamma_i(E_{1m} - E_{0m'}) |M_{mm'}|^2 f_i^0(E_{1m} - E_{0m'}), \quad (5)$$

$$\Gamma_{mm'}^{01} = \sum_{i=L,R} \Gamma_i(E_{1m'} - E_{0m}) |M_{mm'}|^2 \times (1 - f_i^0(E_{1m'} - E_{0m})). \quad (6)$$

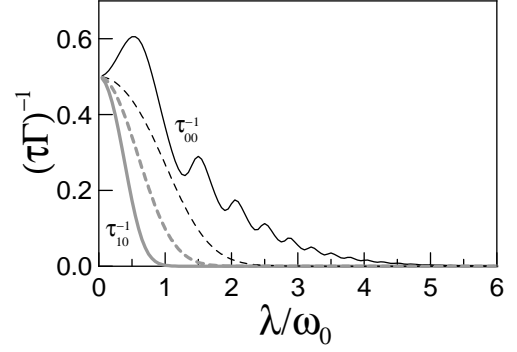


Figure 2: Inverse life-time $(\tau\Gamma)^{-1}$ of the neutral state (thin solid line) and the charged state (thick gray solid line) as a function of λ/ω_0 at $\epsilon_0 = \lambda^2/2\omega_0$; and the same at $\epsilon_0 = 0.9\lambda^2/\omega_0$ (dashed lines), $kT = 0.1\omega_0$.

Here $f^0(\epsilon)$ is the equilibrium Fermi function, and $M_{mm'} = \left\langle 0 \left| \frac{a^m}{\sqrt{m!}} \exp \left[\frac{\lambda}{\omega_0} (a^\dagger - a) \right] \frac{(a^\dagger)^{m'}}{\sqrt{m'!}} \right| 0 \right\rangle$ is the Franck-Condon matrix element. It is symmetric in $m-m'$ and can be calculated analytically. For $m < m'$ it reads

$$M_{m < m'} = \sum_{l=0}^m \frac{(-g)^l \sqrt{m!m'} e^{-g/2} g^{(m'-m)/2}}{l!(m-l)!(l+m'-m)!}, \quad (7)$$

where $g = (\lambda/\omega_0)^2$ is the Huang-Rhys factor [20].

One characteristic feature of these matrix elements in transport is so-called Franck-Condon blockade [18, 19]: in the case of strong electron-vibron interaction the tunneling with small changes in m is suppressed exponentially, as illustrated in Fig. 1(b) for the matrix element $M_{0m} = e^{-g/2} \frac{g^{m/2}}{\sqrt{m!}}$. Hence only tunneling through high-energy states is possible. This is also suppressed at low bias voltage and low temperature.

Finally, the *average charge* is $\langle n \rangle(t) = \sum_m p_{1m}$, and the *average current* (from the left or right lead) reads $J_{i=L,R}(t) = e \sum_{mm'} (\Gamma_{im}^{10} p_{0m'} - \Gamma_{im'}^{01} p_{1m})$.

To proceed further, we calculate the characteristic life times of the neutral and charged ground states. The life time τ_{nm} of the state $|n, m\rangle$ is given by the sum of the rates of all possible processes which change this state, $\tau_{nm}^{-1} = \sum_{n'm'} \Gamma_{m'm}^{n'n}$. As an example, calculating the life time of the neutral state $|0, 0\rangle$, with an energy higher than the charged ground state $|1, 0\rangle$, we find

$$\tau_{00}^{-1} = \sum_m \sum_{i=L,R} \Gamma_i(E_{1m} - E_{00}) |M_{m0}|^2 f_i^0(E_{1m} - E_{00}). \quad (8)$$

For energy-independent Γ_i (the wide-band limit) we obtain the simple analytical expression

$$\tau_{00}^{-1} = \Gamma \sum_m e^{-g} \frac{g^m}{m!} f^0 \left(\epsilon_0 - \frac{\lambda^2}{\omega_0} + \omega_0 m \right). \quad (9)$$

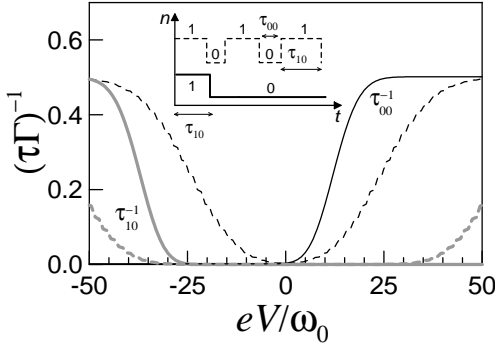


Figure 3: Inverse life-time $(\tau\Gamma)^{-1}$ as a function of normalized voltage eV/ω_0 for the asymmetric junction ($\eta = 0$) at $\lambda/\omega_0 = 5$ and $\epsilon_0 = \lambda^2/2\omega_0$ for the neutral state (thin solid line), the charged state (thick gray solid line) and the same for the symmetric junction ($\eta = 0.5$, dashed lines). Inset: random switching between bistable states (dashed line) and single switching into the stable state (full line) after a sudden change of the voltage.

The corresponding expression for the life time of the charged state is (assuming that the equilibrium electrochemical potential in the leads is zero)

$$\tau_{10}^{-1} = \Gamma \sum_m e^{-g} \frac{g^m}{m!} f^0 \left(-\epsilon_0 + \frac{\lambda^2}{\omega_0} + \omega_0 m \right). \quad (10)$$

The dependence of the tunneling rates (9,10) on the scaled electron-vibron interaction constant λ/ω_0 is shown in Fig. 2. It is clearly seen that at large values of λ the tunneling from the neutral state to the charged state and vice versa is exponentially suppressed in comparison with the bare tunneling rate Γ . Hence both states are (meta)stable at low temperatures and zero voltage.

Based on the experimental parameters of Ref. [2], the charged ground state is assumed to be below the equilibrium Fermi energy of the leads, while the neutral ground state is above it. In the experiments [2] the observed relaxation energy $\epsilon_p \approx 2.4$ eV leads to the parameter λ/ω_0 of the order 5 to 10. Thus the system is in the blockade regime at zero voltage, see Fig. 2.

Next we consider the other important question, whether fast switching between the two states is possible. At finite voltage the switching rates are

$$\tau_{00}^{-1} = \sum_m \frac{e^{-g} g^m}{m!} [\Gamma_L f^0(\epsilon_1 + \omega_0 m - (1-\eta)eV) + \Gamma_R f^0(\epsilon_1 + \omega_0 m + \eta eV)], \quad (11)$$

$$\tau_{10}^{-1} = \sum_m \frac{e^{-g} g^m}{m!} [\Gamma_L f^0(-\epsilon_1 + \omega_0 m + (1-\eta)eV) + \Gamma_R f^0(-\epsilon_1 + \omega_0 m - \eta eV)]. \quad (12)$$

The voltage dependence of the inverse life time $(\tau\Gamma)^{-1}$ is shown in Fig. 3 for a junction with the same tunneling coupling, $\Gamma_L = \Gamma_R$, but asymmetric electrical field

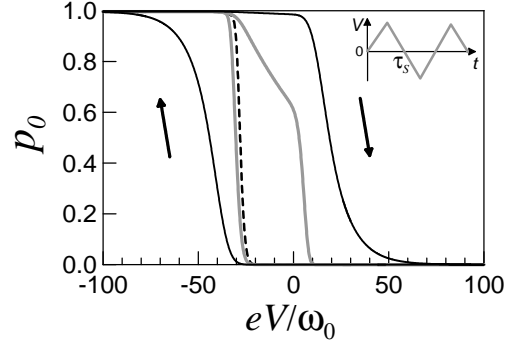


Figure 4: Population of the neutral state as a function of normalized voltage eV/ω_0 in the asymmetrical junction ($\eta = 0$) at $\lambda/\omega_0 = 5$ and $\epsilon_0 = \lambda^2/2\omega_0$ for fast voltage sweep (thin solid line), slower sweep (thick gray solid line), and in the adiabatic limit (dashed line). Inset: sketch of voltage time-dependence.

($\eta = 0$), as well as for the completely symmetric junction ($\eta = 0.5$). The results in Fig. 3 imply that in both cases one can tune $(\tau\Gamma)^{-1}$ upon sweeping the bias voltage and thereby control the timescales for switching between charged and neutral states. For the symmetric junction both switching rates, τ_{00}^{-1} and τ_{10}^{-1} , (dashed lines) are simultaneously nonzero at finite voltage ($eV/\omega_0 \geq 40$ for the parameters of Fig. 3) leading to random switching (noise) sketched as dashed line in the inset. On the contrary, for the asymmetric junction controlled switching into the neutral (black solid line) and charged (grey line) state can be achieved at large enough negative and positive voltage, respectively. This qualitatively different behaviour is a result of the distinct voltage asymmetry of the two inverse lifetimes which are never both finite. The further peculiar feature of the asymmetric case, namely that the switching rates of the neutral and charged states interchange their role as a function of bias, i.e., the neutral (charged) state is long-lived at negative (positive) bias, implies hysteretic behavior and a memory effect.

To this end we consider what happens, if one sweeps the voltage with different velocity (Fig. 4) for the asymmetric case $\eta = 0$. If the voltage is changed fast enough, i.e. faster than the life time of charged and neutral states ($\tau \gg \tau_s$ as discussed in the introduction), then both states can be obtained at zero voltage (hysteresis). In the opposite (adiabatic) limit the change is so slow that the system relaxes into the equilibrium state, and the population-voltage curve is single-valued. Note that this controlled switching is possible only for asymmetric junctions for the reason given above.

We finally compare the results with those of a further important limiting case, namely that the level width is finite (and possible finite dissipation of vibrons is taken into account). Then the master equation approach can no longer be used, and we apply alternatively the nonequilibrium Green function technique. Follow-

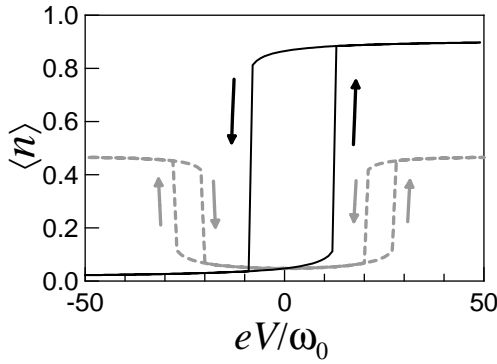


Figure 5: Average number of electrons at $\Gamma_L = \Gamma_R = 5\omega_0$ as a function of normalized voltage eV/ω_0 for the asymmetric junction, $\eta = 0$ (thin solid line), and for the symmetric junction, $\eta = 0.5$ (dashed line), for $\lambda/\omega_0 = 5$ and $\epsilon_0 = \lambda^2/\omega_0$.

ing Refs. [21, 22], the average number of electrons is determined by the lesser Green function $G^<(t_1 - t_2) = i \langle d^\dagger(t_2)d(t_1) \rangle$ as $\langle n \rangle = -i \int G^<(\epsilon) \frac{d\epsilon}{2\pi}$. The calculation of the Green function is a nontrivial task even in the single-level model. It is simplified in the important limit of low vibron frequencies, $\omega_0 \ll \Gamma < \epsilon_p$, where the Born-Oppenheimer approximation holds true. We used the equation-of-motion approach in this case. In Fig. 5 the charge-voltage dependence, obtained in the simplest mean-field approximation [8, 9], is shown. The lesser function is represented as $G^<(\epsilon) = iA(\epsilon)f(\epsilon)$, with the spectral and the distribution function

$$A(\epsilon) = \frac{2\Gamma}{(\epsilon - \epsilon_0 - \frac{2\lambda^2}{\omega_0} \langle n \rangle - e\varphi_0)^2 + \Gamma^2}, \quad (13)$$

$$f(\epsilon) = \frac{\Gamma_L f_L^0(\epsilon - e\varphi_L) + \Gamma_R f_R^0(\epsilon - e\varphi_R)}{\Gamma_L + \Gamma_R}. \quad (14)$$

The result is qualitatively the same as in the sequential tunneling case: For electrically asymmetric junctions two stable states exist at zero bias (memory effect), which can be switched by the voltage. The current shows similar hysteretic behaviour as a function of voltage. For the symmetric junction hysteresis is observed only at finite voltage (nonequilibrium bistability [9]). Hence, asymmetric junctions are again preferable for a memory effect.

Finally we note that in the case $\omega_0 \ll \Gamma$ we considered the stationary problem only, assuming that the switching rate between the two metastable states is small (compared e.g. to Γ) at large λ/ω_0 . The calculation of the life times of metastable states within the Green function approach and of dynamical effects arising from the competition between voltage sweeping and switching times, such as in Fig. 4, remains as a problem for the future.

To conclude, we considered a *charge-memory effect* and switching phenomena in single-molecule junctions taking into account dynamical effects such as the interplay between timescales of voltage sweeping and switching rates.

We showed that bistability arises if quantum transitions between neutral and charged states involved are suppressed, e.g. due to Franck-Condon blockade. Different regimes, characterized by random mutual transitions and by single switching events into a stable configuration are identified. In the latter case controlled switching of the molecule is achieved by applying finite voltage pulses.

We acknowledge fruitful discussions with J. Repp. This work was funded by the Deutsche Forschungsgemeinschaft within the Priority Program SPP 1243 and Collaborative Research Center SFB 689 (D.A.R.).

-
- [1] A. S. Alexandrov and A. M. Bratkovsky, Phys. Rev. B **67**, 235312 (2003).
 - [2] J. Repp, G. Meyer, F. E. Olsson, and M. Persson, Science **305**, 493 (2004).
 - [3] F. E. Olsson, S. Paavilainen, M. Persson, J. Repp, and G. Meyer, Phys. Rev. Lett. **98**, 176803 (2007).
 - [4] E. Lörtscher, H. B. Weber, and H. Riel, Phys. Rev. Lett. **98**, 176807 (2007).
 - [5] P. Liljeroth, J. Repp, and G. Meyer, Science **317**, 1203 (2007).
 - [6] M. del Valle, R. Gutiérrez, C. Tejedor, and G. Cuniberti, Nature Nanotechnology **2**, 176 (2007).
 - [7] G. Cuniberti, G. Fagas, and K. Richter, *Introducing Molecular Electronics* (Springer-Verlag, 2005).
 - [8] A. C. Hewson and D. M. Newns, J. Phys. C: Solid State Phys. **12**, 1665 (1979).
 - [9] M. Galperin, M. A. Ratner, and A. Nitzan, Nano Lett. **5**, 125 (2005).
 - [10] A. Mitra, I. Aleiner, and A. J. Millis, Phys. Rev. Lett. **94**, 076404 (2005).
 - [11] D. Mozyrsky, M. B. Hastings, and I. Martin, Phys. Rev. B **73**, 035104 (2006).
 - [12] S. Datta, W. Tian, S. Hong, R. Reifenberger, J. I. Henderson, and C. P. Kubiak, Phys. Rev. Lett. **79**, 2530 (1997); T. Rakshit, G.-C. Liang, A. W. Gosh, M. C. Hersam, and S. Datta, Phys. Rev. B **72**, 125305 (2005).
 - [13] I. G. Lang and Y. A. Firsov, Sov. Phys. JETP **16**, 1301 (1963).
 - [14] A. C. Hewson and D. M. Newns, Japan. J. Appl. Phys. Suppl. **2**, Pt. **2**, 121 (1974).
 - [15] G. Mahan, *Many-Particle Physics* (Plenum, N. Y., 1990).
 - [16] S. Braig and K. Flensberg, Phys. Rev. B **68**, 205324 (2003).
 - [17] A. Mitra, I. Aleiner, and A. J. Millis, Phys. Rev. B **69**, 245302 (2004).
 - [18] J. Koch and F. von Oppen, Phys. Rev. Lett. **94**, 206804 (2005); J. Koch, M. Semmelhack, F. von Oppen, and A. Nitzan, Phys. Rev. B **73**, 155306 (2006).
 - [19] K. C. Nowack and M. R. Wegewijs, cond-mat/0506552.
 - [20] K. Huang and A. Rhys, Proc. R. Soc. London Ser. A **204**, 406 (1950).
 - [21] Y. Meir and N. S. Wingreen, Phys. Rev. Lett. **68**, 2512 (1992); A.-P. Jauho, N. S. Wingreen, and Y. Meir, Phys. Rev. B **50**, 5528 (1994).
 - [22] H. Haug and A.-P. Jauho, *Quantum Kinetics and Optics of Semiconductors*, vol. 123 of *Springer Series in Solid-State Sciences* (Springer, 1996).